18

More on unpolarized deep inelastic scatterings

18.1 Target mass corrections

Target mass corrections have been introduced by Nachtmann [229], and later on in [168]. If one considers the NS part of the moments defined in Eq. (16.16), one can show [168] that they can be written as:

$$\mathcal{M}_2^{(n)}(Q^2)\big|_{\text{mass}} = \sum_{j=0}^{\infty} \left(\frac{M_N^2}{Q^2}\right)^j \frac{(n+j)!}{j!(n-2)!(n+2j)(n+2j-1)} \mathcal{M}_2^{(n)}(Q^2)\,. \quad (18.1)$$

Inverting this expression, one can express the structure function in terms of the Nachtmann variable [229]:

$$\zeta = \frac{2x}{1+\sqrt{1+4x^2M_N^2/Q^2}}\,. \quad (18.2)$$

In the region $x \to 1$, higher twist contributions can also be important and can cancel the target mass corrections [230], it is instructive to do an expansion in x. Keeping the leading term, one obtains (see e.g. [46]):

$$\begin{aligned} F_2^{NS}\big|_{\text{mass}}(x,Q^2) = F_2^{NS}(x,Q^2) + \frac{x^2M_N^2}{Q^2} \\ \times \left\{6x\int_0^1 \frac{dy}{y^2}\, F_2^{NS}(y,Q^2) - \frac{x\partial F_2^{NS}(x,Q^2)}{\partial x} - 4F_2^{NS}(x,Q^2)\right\} \\ + \mathcal{O}\left((3\sim 5)\frac{x^3M_N^2}{(1-x)Q^2}\right)\,, \end{aligned} \quad (18.3)$$

where the quality of the expansion can be controlled by the size of the next term. This contribution can be compared with the higher-twist contribution in Eq. (18.6).

18.2 End points behaviour and the BFKL pomeron

18.2.1 The limit $x \to 1$

The NLO perturbative expression of the non-singlet structure function indicates that for $x \to 1$, it behaves as [231]:

$$F^{NS} \sim (1-x)^{2[\ln(1-x)](\alpha_s/3\pi)}\,, \quad (18.4)$$

https://doi.org/10.1017/9781009290296.026 Published online by Cambridge University Press

showing that perturbation theory fails. This result can be generalized to all orders by formally replacing $\alpha_s(Q^2)$ by $\alpha_s[(1-x)Q^2]$ [241]. One can also interpret this feature because, in this limit, we are in the bound state regime where the reaction of the type:

$$\gamma^* + N \to N \tag{18.5}$$

dominates. In this limit, one may also expect that non-perturbative higher twist contributions behave as [230]:

$$F_2^{HT}(x, Q^2) \sim \frac{p_T^2}{Q^2} \frac{x}{1-x} F_2(x, Q^2) \,, \tag{18.6}$$

where p_T is the transverse momentum of partons in the nucleon.

18.2.2 The limit $x \to 0$ for the non-singlet case

This limit has been studied extensively in hadron physics for the non-singlet scattering process.[1] It corresponds to the kinematic region where Q^2 is fixed and the hadronic energy ν going to infinity. This is the so-called *Regge limit*, where the cross-section of the photon scattering off the proton is proportional to the structure function:

$$\sigma(\gamma^*(Q^2)p(s)) = \frac{4\pi^2\alpha}{Q^2} F_2(x, Q^2) \;: \qquad s = Q^2/x \,, \tag{18.7}$$

and where the non-singlet amplitude can be expressed as:

$$T^{NS}(\nu \to \infty) \simeq f(Q^2) s^{\alpha_\rho(0)} \,, \tag{18.8}$$

due to exhange of Regge trajectories, either the ρ trajectory or the one degenerate to it. $\alpha_\rho(0)$ is the *universal intercept* of the ρ trajectory, which has an experimental value of about 0.5. Therefore, one can show that the structure function behaves as:

$$F_2^{NS}(x, Q^2) \sim x^{1-\alpha_\rho(0)} \,. \tag{18.9}$$

18.2.3 The limit $x \to 0$ for the singlet case and the BFKL pomeron

The singlet case is more subtle due to the coupled evolution equations from the presence of the gluon density. At present, there is no consensus on the behaviour of the structure functions at $Q_0^2 \sim$ few GeV^2. There are three proposals:

- **Soft pomeron**
  In this case, the structure functions are expected to behave as a constant in the $x = 0$ limit. This behaviour was first considered in [230] and completed later on. However, it has been known for a long time that a soft pomeron for off-shell processes leads to inconsistencies [243].
- **Hard pomeron**
  The previous remark then leads some people to postulate the hard pomeron exchange, where:

$$F^S\left(x, Q_0^2\right) \sim x^{-\lambda_q} \,, \qquad F^G\left(x, Q_0^2\right) \sim x^{-\lambda_g} \,. \tag{18.10}$$

[1] For a recent review, see e.g. [242].

https://doi.org/10.1017/9781009290296.026 Published online by Cambridge University Press

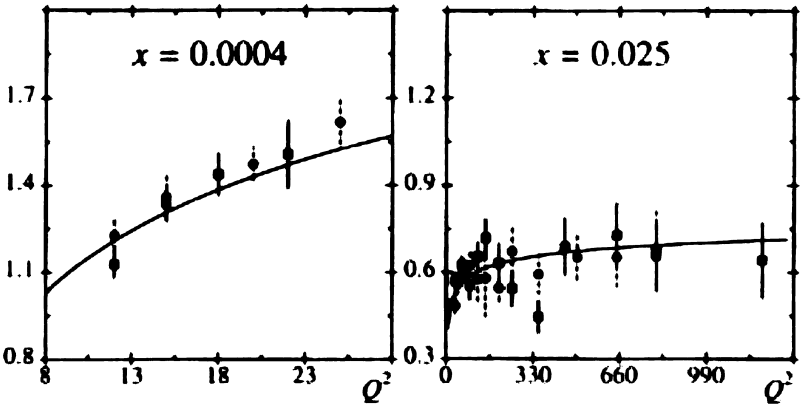

Fig. 18.1. Comparison of the measured and BFKL predictions of F_2 for small $x = 4 \times 10^{-4}$ and large Q^2. For a running value of α_s, the HERA data are in disagreement with the BFKL result (F_2 should decrease with Q^2).

It has been proved that:

$$\lambda_q = \lambda_g \tag{18.11}$$

and are Q^2 independent.

- **BFKL pomeron**

  The usual procedure used now is to assume a given behaviour at fixed Q_0^2 and then evolve the behaviour using the RGE for an arbitrary Q^2. Using a different approach, BFKL [244] found a different behaviour:

$$F_2\big(x, Q^2\big) \sim x^{-\omega\alpha_s(Q^2)} \ : \qquad \omega = \frac{4C_A \ln 2}{\pi} \ . \tag{18.12}$$

  which is not compatible with the RGE where the exponent is constant. A comparison of this prediction with data for a given small x value is given in Fig. 18.1.

  A number of speculations have been suggested in order to explain this difference (two different regimes in x ? α_s function of a soft scale of the order of Λ^2 but not of Q^2 ? . . .).

18.3 Experimental tests and new developments

- In the previous section, we have discussed in detail the scaling violation to the Bjorken sum rule as an illustration of the OPE approach and of the Altarelli–Parisi evolution equation. We have also concentrated the discussions on the photon scattering off a proton. A test of this prediction is given in Fig. 18.2.

  We also give the new compiled data from PDG [16] in Figs. 18.3 and 18.4.
- In [245], a model which interpolates the soft and hard pomeron parametrization and which can be used at low Q^2 has been proposed. It has been assumed that the soft pomeron contribution is given by an ordinary pomeron which is constant when $x \to 0$, while one has to find a parametrization

https://doi.org/10.1017/9781009290296.026 Published online by Cambridge University Press

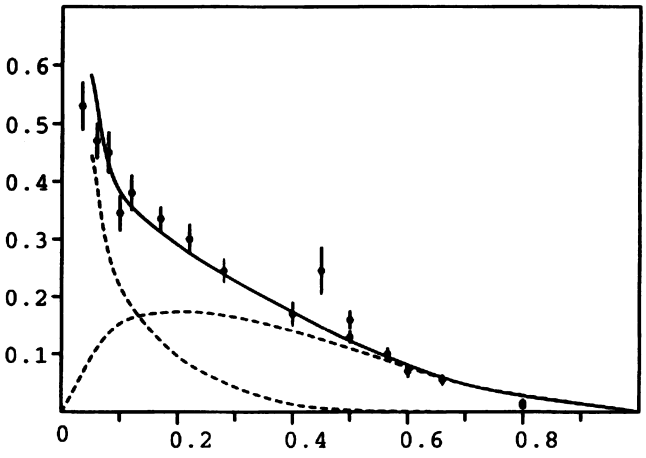

Fig. 18.2. Comparison of the measured and QCD predictions for F_2 where the NS and S components (dashed) are explicitly shown. The full curve is the sum of the two. Data points are SLAC data [246].

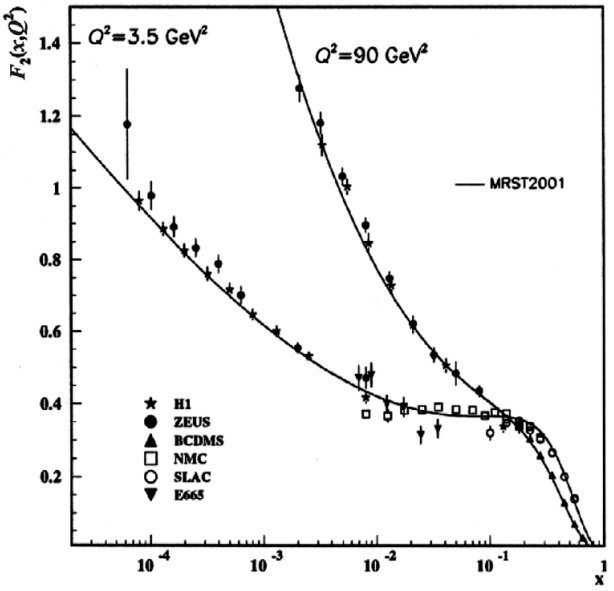

Fig. 18.3. The proton structure function F_2 from ep scattering versus x at two values of Q^2, exhibiting scaling at the pivot point $x \approx 0.14$.

where the cross-section does not blow up when $Q^2 \to 0$. This can be achieved by replacing the coupling by:

$$\alpha_s(Q^2) \to \tilde{\alpha}_s \equiv \frac{2\pi}{-\beta_1 \ln(Q^2 + M^2)/\Lambda^2}\,, \tag{18.13}$$

https://doi.org/10.1017/9781009290296.026 Published online by Cambridge University Press

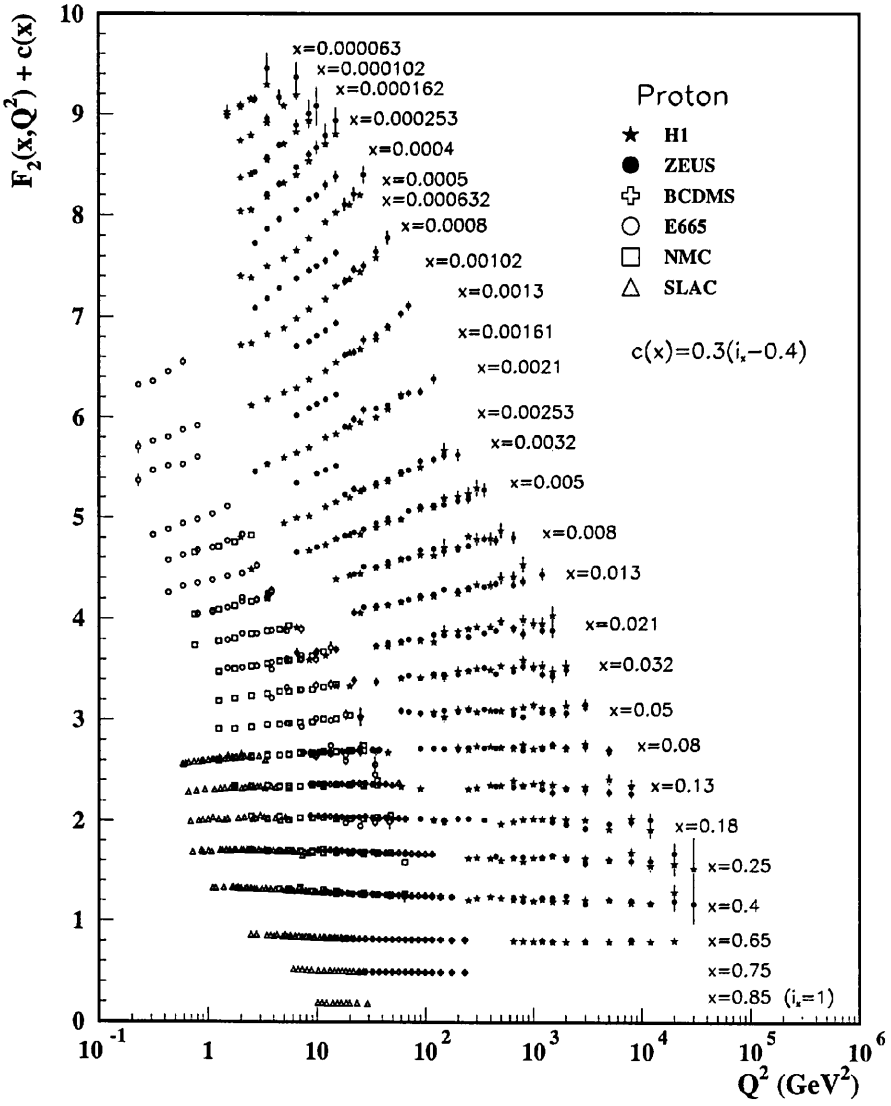

Fig. 18.4. The proton structure function F_2 from ep scattering versus Q^2 at different values of x. A constant $c(x) = 0.3(i_x - 0.4)$ has been added to F_2 where i_x is the number of the x bin ranging from $i_x = 1(x = 0.85)$ to $i_x = 28(x = 0.000063)$.

and the soft pomeron term by:

$$C \to C \frac{Q^2}{Q^2 + M^2} , \tag{18.14}$$

where M is a typical hadronic scale of the order of M_ρ. In this way, the structure function takes the form:

$$F_2 = \langle e_q^2 \rangle B_S \tilde{\alpha}_s^{-d^+(n=1+\lambda)} Q^{-2\lambda} s^\lambda + C \frac{Q^2}{Q^2 + M^2} + B_{NS} \tilde{\alpha}_s^{-d^{NS}(n=1-\lambda_{NS})} Q^{2\lambda^{NS}} s^{-\lambda^{NS}} , \tag{18.15}$$

https://doi.org/10.1017/9781009290296.026 Published online by Cambridge University Press

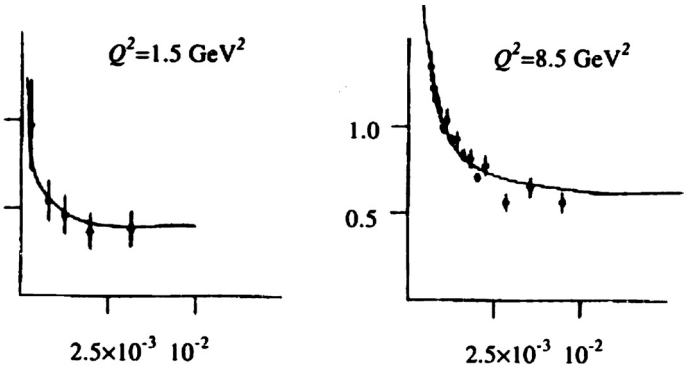

Fig. 18.5. Comparison of the measured and QCD model predictions for F_2 at low x and small Q^2.

with:

$$d_+(1+\lambda_0) = 1+\lambda_0\,, \qquad d^{NS}\left(1-\lambda_0^{NS}\right) = 1-\lambda_0^{NS}\,, \tag{18.16}$$

and:

$$d(n) \equiv \gamma_n/(-2\beta_1)\,. \tag{18.17}$$

The different fits give a good description of the HERA data at low x and small Q^2, as shown in Fig. 18.5.

The results of the fit give:

$$\lambda_0 = 0.47\,, \qquad \lambda_0^{NS} = 0.522\,. \tag{18.18}$$

which are larger than a hard pomeron fit $\lambda = 0.32 - 0.38$ but are in the range given by a soft pomeron fit $\lambda = 0.44 \pm 0.04$.

- We also know that deep inelastic scatterings and some other related sum rules have been traditionally used for extracting the QCD coupling $\alpha_s(Q^2)$ and the scale Λ due to their sensitivity to leading order to these quantities. The determinations of α_s from different methods will be discussed in Section 18.4, Chapter 25 and Part VI. Various more involved systematic tests of scaling violations and modern analysis can, for example, be found in different textbooks [42–46], reviews [47–52] and also the proceedings of the QCD series of the Montpellier-Conference.

18.4 Neutrino scattering sum rules

For (anti)-neutrino off-proton scattering, we have the following sum rules:

- **The Adler sum rule**

$$\int_0^1 \frac{dx}{x}\left(F_2^{\bar{\nu}p} - F_2^{\nu p}\right) = 2\,, \tag{18.19}$$

valid for all Q^2, and which has no corrections because it is related to an equal-time commutator [247].

https://doi.org/10.1017/9781009290296.026 Published online by Cambridge University Press

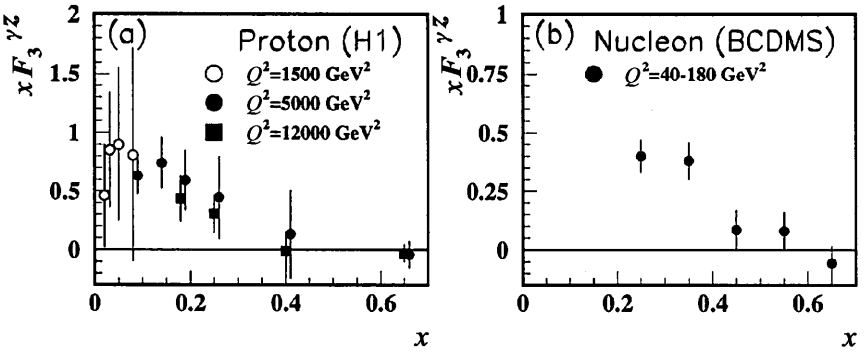

Fig. 18.6. xF_3 measured from electroweak scattering of (a) electrons on protons and (b) muons on carbon versus x and for different Q^2.

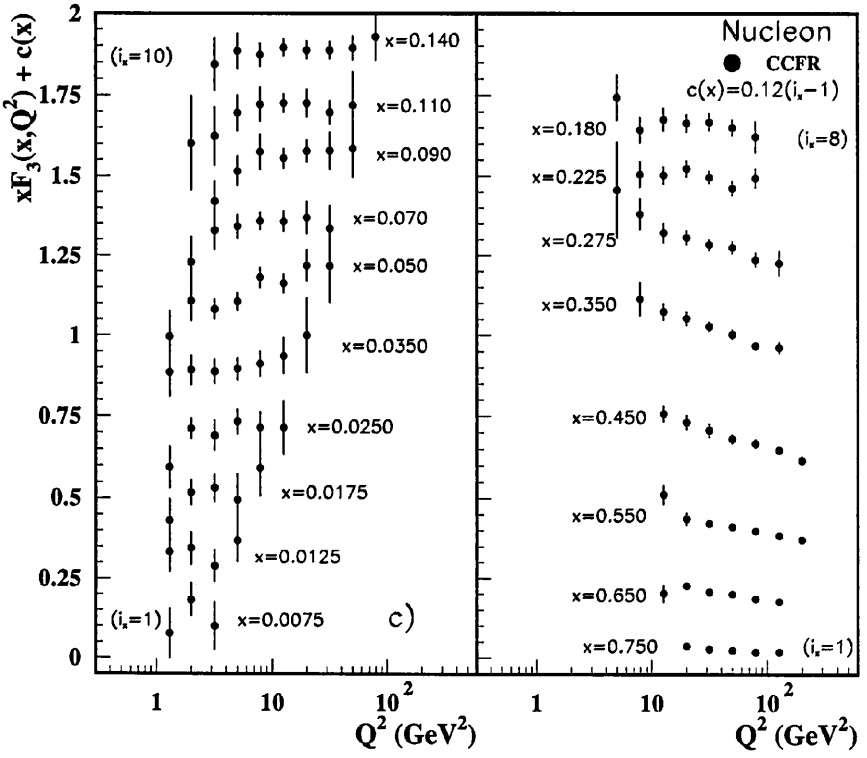

Fig. 18.7. xF_3 measured from $\nu - Fe$ scattering versus Q^2 and for different x.

https://doi.org/10.1017/9781009290296.026 Published online by Cambridge University Press

- **The Gross–Llewellyn Smith sum rule**
  It reads [248]:

$$\int_0^1 \frac{dx}{x}\left[F_3^{\bar{\nu}p}(x,Q^2)+F_3^{\nu p}(x,Q^2)\right]=3\left\{1-a_s(Q^2)-3.58\,a_s^2(Q^2)-19.0\,a_s^3(Q^2)\right\}, \quad (18.20)$$

  where higher order corrections have been evaluated by [249] and are shown in Fig. 18.6.
  Data [16] from ν-Fe scattering is shown in Fig. 18.7.

18.5 Summary of α_s measurements from DIS

The different analysis from DIS lead to the values of α_s given in Table 25.3 and Fig. 25.13 from [139]. The most recent and precise result comes from the analysis of F_2 by [250] using data on protons from SLAC, BCDMS, E665 and HERA. It leads to:

$$\alpha_s(M_{Z^0}) = 0.1166 \pm 0.0009\ (\text{stat}) \ \pm 0.0020\ (\text{syst})\ , \quad (18.21)$$

where the systematic error has been multiplied by a factor 2 as a guess of the μ-dependence and effects of power corrections not fully analysed in [250]. It reaches the accuracy of the determination from, for example, the inclusive τ-decay data. However, the DIS data have shown large fluctuations in recent years, and then are less satisfactory than those from e^+e^- and τ-decay data. The previous value $\alpha_s(M_{Z^0}) = 0.113 \pm 0.005$ from BCDMS, SLAC data [251] and soon confirmed by the CCFR result from $F_{2,3}$, become 0.119 ± 0.002 (stat) $\pm$ 0.003 (th) after a new energy calibration. Recent result on $F_2\gamma$ photon structure function is also available from LEP leading to:

$$\alpha_s(M_{Z^0}) = 0.1198 \pm 0.0028\ (\text{exp})\ ^{+0.0034}_{-0.0046}\ (\text{th})\ . \quad (18.22)$$

These different DIS results are compared with other determinations given in Table 25.3 and Figs. 25.13 and 25.15. The overall agreement shows a great achievement of the pQCD calculations.

https://doi.org/10.1017/9781009290296.026 Published online by Cambridge University Press